phys. stat. sol. (a) **188**, No. 2, 751–755 (2001)

Three-Dimensional Imaging of ELOG Growth Domains by Scanning Cathodoluminescence Tomography

T. RIEMANN[1]) (a), J. CHRISTEN (a), A. KASCHNER (b), A. HOFFMANN (b), C. THOMSEN (b), M. SEYBOTH (c), F. HABEL (c), R. BECCARD (d), and M. HEUKEN (d)

(a) Institute of Experimental Physics, Otto-von-Guericke-University, PO Box 4120, D-39016 Magdeburg, Germany

(b) Institute of Solid State Physics, Technical University Berlin, Germany

(c) Optoelectronics Department, University of Ulm, Germany

(d) AIXTRON AG, Aachen, Germany

(Received June 25, 2001; accepted July 11, 2001)

Subject classification: 61.72.Ss; 78.30.Fs; 78.60.Hk; S7.14

Columnar ELOG growth domains formed in a 65 μm thick HVPE GaN layer during overgrowth of hexagonal SiO_2 masks are three-dimensionally characterized using spatially and spectrally resolved scanning cathodoluminescence (CL) microscopy. In conjunction with cross-sectional imaging perpendicular to the *c*-plane, a direct visualization of the 3D domain formation is achieved by consecutive vertical series of CL mappings parallel to the *c*-plane. A perfect agreement between the local luminescence properties and the evolution of the local free carrier concentration during the different stages of overgrowth is confirmed by micro-Raman measurements. While mask-periodic domains with specific optical and electronic properties are observed for initial growth, homogeneously high crystal quality at the sample surface is evidenced.

Introduction Cathodoluminescence (CL) microscopy has proven its immense potential to characterize the evolution of the epitaxial lateral overgrowth of GaN (ELOG), evidencing the formation of specific growth domains with typical properties for a variety of mask patterns and growth conditions [1–4]. In these investigations, 2D imaging was performed either on cleaved faces perpendicular to the *c*-plane or on the as-grown sample surface. While this method is appropriate for ELOG on stripe masks, it only gives incomplete information for grid-like mask patterns. One approach to perform 3D characterization is to consecutively remove the ELOG layer to clearly defined depths [5]. In this paper we present such a full 3D characterization of columnar ELOG domains formed during overgrowth of hexagonal masks.

Experimental Following the deposition of a 2 μm MOVPE buffer on (0001) sapphire substrate, a SiO_2 layer was patterned by photolithography and wet chemical etching into a periodic mask of 7 μm wide SiO_2 hexagons set 11 μm apart. Subsequently, these patterned templates were overgrown in an AIXTRON horizontal HVPE system. In conjunction with our 'standard' cross-sectional CL imaging at cleaved faces perpendicular to the *c*-plane, a direct visualization of the 3D domain formation in the HVPE layer is achieved by consecutive vertical series of mappings parallel to the *c*-plane. For these depth-resolved CL investigations a 2.4 mm wide spherical pit was fabricated in the

[1]) Phone: +49 391 67 11259; Fax: +49 391 67 11130;
e-mail: till.riemann@student.uni-magdeburg.de

 0031-8965/01/18811-0751 $ 17.50+.50/0

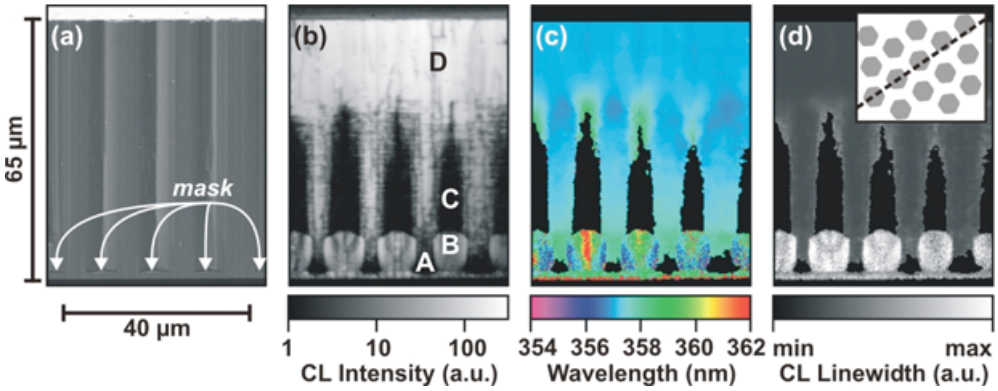

Fig. 1. Cross-sectional SEM and CL mappings (T = 5 K) perpendicular to the sample c-plane

ELO-GaN by mechanical grinding and polishing, reaching through the MOVPE buffer layer at its very center. The pit profile was determined using a surface profiler, establishing the correlation between depth and lateral position. CL maps were taken at different lateral positions with respect to the pit center, leading to a series of cross-sectional images almost parallel to the c-plane but at increasing c-position ranging from the buffer layer up to the ELOG surface. For 50 µm wide maps used here, the spherical inclination of the pit slopes results in a depth difference, which is well below 1 µm in the mask plane and about 5 µm directly underneath the sample surface. Details of the scanning electron microscope (SEM) based low temperature CL setup and the µ-Raman technique for determining the local free carrier concentration are given in [3].

Results and Discussion Figure 1 shows cross-sectional mappings of the ELOG layer perpendicular to the c-plane. While at the left-hand side of these images the cleaved face almost crosses the centers of the hexagonal masks, at the right-hand side only the mask edges are met. This is illustrated in the schematic mask pattern depicted in the inset of Fig. 1d.

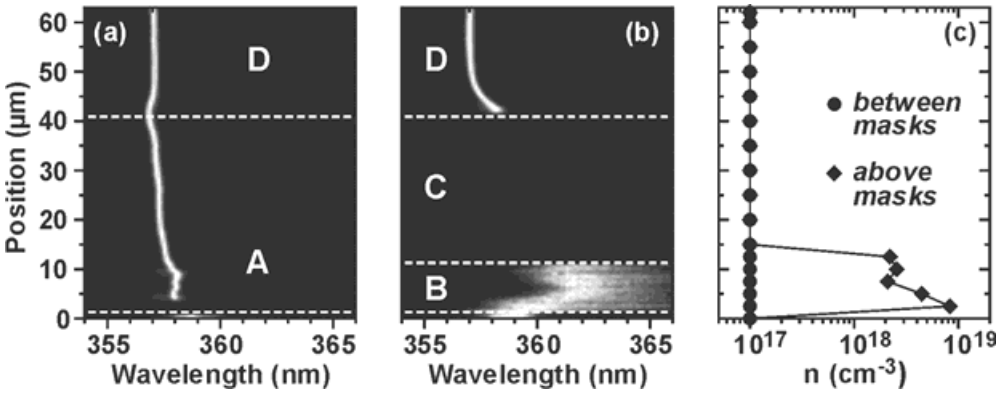

Fig. 2. Evolution of luminescence and local free carrier concentration n parallel to the c-axis

The SEM image Fig. 1a shows an almost homogeneous structure with a weak columnar corrugation along the *c*-axis. In strong contrast, a variety of distinct features showing characteristic luminescence properties are visible in the integral CL intensity image (CLI) of the Near Bandedge emission Fig. 1b, the CL wavelength image (CLWI) Fig. 1c, as well as in the mapping of the CL linewidth Fig. 1d; all four displaying the identical area. These features directly correspond to specific growth domains formed during the evolution of the ELO GaN, marked in Fig. 1b. Initial (0001) growth in the unmasked areas (A) is characterized by sharp, however, weak excitonic emission, indicating a low impurity incorporation but high density of non-radiative recombination centers near the MOVPE/HVPE GaN interface. Directly underneath the mask-openings even the luminescence of the buffer is affected, showing an abrupt drop of quantum efficiency. With advancing (0001) growth the excitonic emission intensity above the unmasked areas gradually increases. A high density of dark lines running parallel to the mask plane is visible in the CL intensity image Fig 1b in this area. These lines of low quantum efficiency directly visualize dislocations bent perpendicular to the growth direction. The onset of facetted overgrowth (B) at the mask edges coincides with a drastic increase of integral CL intensity. This high integral intensity is exclusively caused by the appearance of broad (Fig. 1d) and blue shifted (Fig. 1c) (e, h)-plasma luminescence, indicating a high local free carrier concentration *n*. The following lateral expansion of

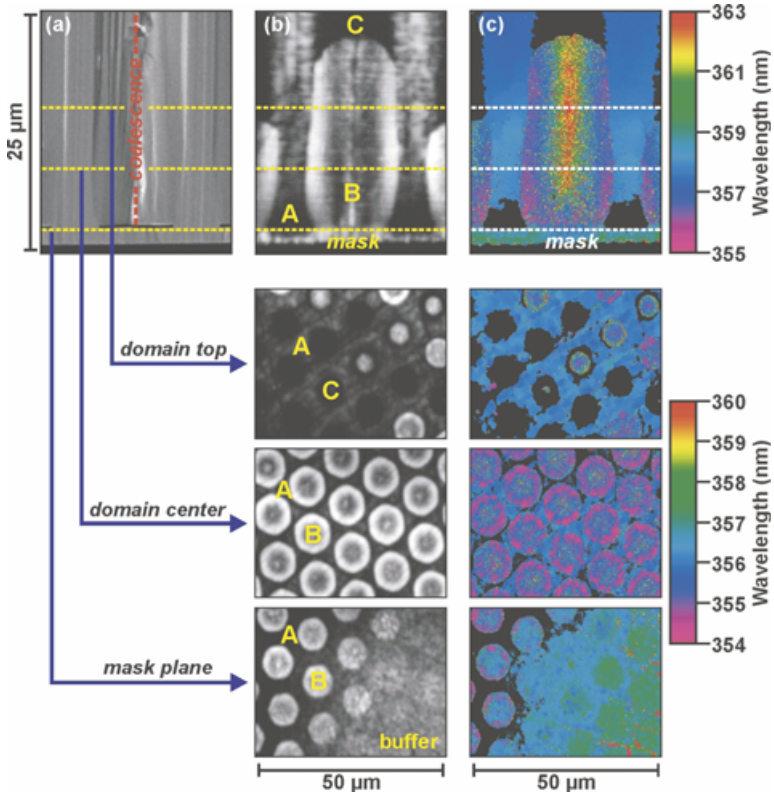

Fig. 3. Three-dimensional CL characterization (T = 5 K) of columnar ELOG domains

the ELO GaN is accompanied by a gradual redshift of the plasma edge, i.e. a monotonous decrease of n. In the coalescence region directly above the mask centers we preferentially find extrinsic luminescence which is consistent with a strong impurity incorporation. While the (0001) growth in A uninhibitedly extends up to the sample surface, the characteristic properties of B are restricted to self-limited columns with an average height of 10 μm. Following a totally self-organized transition, further growth above the masks leads to an abrupt drop of the near band-edge CL in 30 μm high cone-shaped domains C (Fig 1b). Exactly here we preferentially find yellow luminescence. In the final domain of 15 μm (0001) growth above and between the masks (D), no influence of the actual mask positions on the bright excitonic emission is found by CL, evidencing a homogeneously high quality of this upper layer.

Using μ-Raman mappings to directly determine n, we find a perfect agreement between the optical and electrical properties. In Fig. 2, CL line scans parallel to the c-axis (bright contrast means high CL intensity) are compared with the corresponding evolution of n.

The CL line scan Fig. 2a, running through a mask opening, is always dominated by the sharp excitonic emission found in A and D. In Fig. 2c the corresponding n never exceeds the detection limit of 10^{17} cm^{-3}. In total contrast, we observe an extremely high n reaching 10^{19} cm^{-3} directly above the masks, exactly where the CL line scan Fig. 2b exhibits the broad luminescence band inside B. Where the broad CL vanishes at the transition to C, n abruptly drops below the detection limit. Region D is characterized by sharp excitonic emission and a low n also above the masks. In these cross-sectional investigations the shape of the columnar ELOG domains A, B and C depends on the actual orientation of the cleaved face. A complete 3D image is obtained by additional depth-resolved mappings parallel to the to the c-plane. In Fig. 3 a consecutive series of such CLI and CLWI mappings near the mask plane is displayed. The vertical sampling positions of these mappings are indicated in the cross-sectional SEM image (Fig. 3a), CLI (Fig. 3b), and CLWI (Fig. 3c) shown above. Due to the slight inclination, both, the upper part of the buffer and the onset of the HVPE growth are visible in the lowest row of Fig. 3. The high defect density of the buffer layer is illustrated by red shifted CL and a high density of dark spots visualizing the drop of quantum efficiency around dislocations. Directly above the MOVPE/HVPE interface, the grid-like pattern of A interchanges with the hexagonal shapes of B. In the middle row, the high integral CL intensity and blue shifted position of the (e, h)-plasma luminescence inside B is clearly visualized in ring-like structures appearing in the CLI and CLWI, respectively. In the upper row, above some mask hexagons the very tops of B are still seen, while at other mask positions the transition to C has already occurred.

Conclusion Columnar ELOG domains formed during HVPE overgrowth of hexagonal SiO_2 masks were 3D imaged by CL microscopy. The areas of initial (0001) growth between the masks show sharp excitonic luminescence and a local free carrier concentration n well below 10^{17} cm^{-3}. The first stage of facetted lateral overgrowth leads to 10 μm high self-limited columns exhibiting broad (e, h)-plasma CL above the mask edges, extrinsic luminescence in the coalescence areas, and n reaching 10^{19} cm^{-3}. Subsequent growth above the masks results in an abrupt drop of n below 10^{17} cm^{-3} inside 30 μm high cones emitting yellow CL. The final ELOG domain (uppermost 15 μm) is completely dominated by excitonic CL above and between the masks, indicating a homogeneously high crystal quality at the sample surface.

Acknowledgement This work is supported by the Deutsche Forschungsgemeinschaft (CH 87/4-2, Tho662/4-2).

References

[1] F. BERTRAM, T. RIEMANN, J. CHRISTEN, A. KASCHNER, A. HOFFMANN, C. THOMSEN, K. HIRAMATSU, T. SHIBATA, and N. SAWAKI, Appl. Phys. Lett. **74**, 359 (1999).
[2] A. KASCHNER, A. HOFFMANN, C. THOMSEN, F. BERTRAM, T. RIEMANN, J. CHRISTEN, K. HIRAMATSU, T. SHIBATA, and N. SAWAKI, Appl. Phys. Lett. **74**, 3320 (1999).
[3] A. KASCHNER, A. HOFFMANN, C. THOMSEN, F. BERTRAM, T. RIEMANN, J. CHRISTEN, K. HIRAMATSU, H. SONE, and N. SAWAKI, Appl. Phys. Lett. **76**, 3418 (2000).
[4] T. RIEMANN, J. CHRISTEN, A. KASCHNER, A. HOFFMANN, C. THOMSEN, O. PARILLAUD, V. WAGNER, and M. ILEGEMS, in: Proc. of the IWN2000, IPAP Conf. Series **1**, 475 (2000).
[5] S. DASSONNEVILLE, A. AMOKRANE, B. SIEBER, J.L. FARVACQUE, B. BEAUMONT, G. GIBART, J.-D. GANIERE, and K. LEIFER, J. Appl. Phys. **89**, 7966 (2001).